Int. J. Heat Mass Transfer. Vol. 22, pp. 901–907
© Pergamon Press Ltd. 1979. Printed in Great Britain

0017-9310/79/0601-0901 $02.00/0

HEAT TRANSFER DURING PISTON COMPRESSION INCLUDING SIDE WALL AND CONVECTION EFFECTS

R. GREIF, T. NAMBA* and M. NIKANHAM†
Department of Mechanical Engineering and Lawrence Berkeley Laboratory,
University of California, Berkeley 94720, U.S.A.

(*Received* 30 *June* 1978 *and in revised form* 16 *November* 1978)

Abstract—The unsteady heat flux from a non-reacting gas to the sidewalls of a channel has been determined during the piston compression of a single stroke. For small changes in the wall temperature, the heat flux may be determined solely from the variation of the temperature outside the boundary layer or, alternatively, from the piston trajectory. Results for the heat-transfer coefficient are also presented and exhibit a non-monotonic variation with respect to time.

NOMENCLATURE

c, specific heat of solid;
c_p, specific heat of gas;
h, heat-transfer coefficient;
k, thermal conductivity;
p, gas pressure;
q, heat flux;
R, gas constant;
t, time;
T, temperature;
u, gas velocity in x direction;
V, volume;
x, coordinate normal to wall;
y, coordinate parallel to wall.

Greek symbols

α, $k/\rho c_p$ thermal diffusivity;
γ, ratio of the specific heats;
δ_{th}, thermal boundary-layer thickness;
Θ, $\left(\frac{T}{T_\infty}\right)^2$;
v, gas velocity in y direction;
ϕ, $\frac{T}{T_\infty}$;
ρ, density;
ψ, stream coordinate;
τ, transformed time.

Subscripts

g, gas;
i, initial;
no conv, no convection;
s, solid;
w, wall;
∞, outside boundary layer.

INTRODUCTION

THE STUDY of the heat transfer from a gas to the walls during piston compression has been the subject of many investigations [1–6]. Unfortunately, the transient, variable volume, variable pressure nature of the compression process results in complex effects that are difficult to isolate and appraise. Accordingly, in an earlier work we studied the heat transfer from a transparent non-reacting gas to the end wall of a channel during the piston compression of a single stroke [7]. This eliminated expansion effects, radiation contributions, cyclical variations, etc. The present work considers the heat transfer to the side walls and also appraises and elucidates the importance of the various transport contributions. A specification of the wall heat flux is also made based solely on the piston trajectory.

EXPERIMENTAL APPARATUS AND MEASUREMENTS

A detailed description of the system and measurements is available [7, 8] and only a brief coverage is given here. The apparatus used was a stainless steel enclosure that was fitted with a pneumatically operated piston. The square compression chamber or test section, 3.8 × 3.8 cm in cross-section, contained an aluminum piston that was fitted with teflon seals. A typical stroke for the experiment was 12 cm with a compression ratio of 4 and a time interval of 30 ms.

A steel rod which moved with the piston was fitted with a steel rack with a set of teeth. A magnetic pickup sensed the teeth as they passed by and the corresponding change in voltage, recorded as a function of time (cf. Fig. 1), yielded the piston displacement. The pressure was determined from the output of a Kistler pressure transducer, SN 52036 (cf. Fig. 1).

To determine the heat flux a thin film resistance thermometer was used [4, 7, 9–18]. It consisted of a thin platinum film that was painted and baked on a ceramic base, Macor, made by Corning Glass

*Present address: Nippon Steel Corporation, Tokyo, Japan.
†Present address: Union Carbide Corporation, Bound Brook, New Jersey, U.S.A.

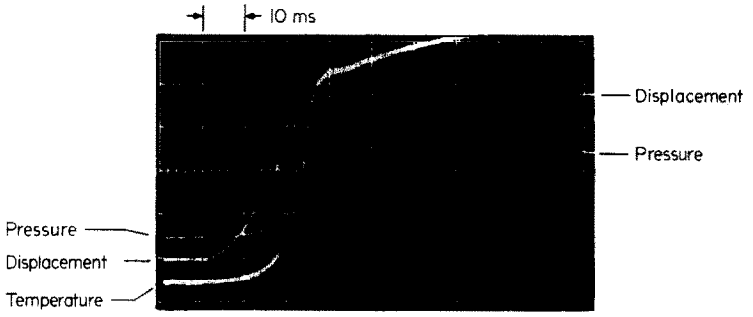

FIG. 1. Typical oscillogram for surface temperature, displacement and pressure measurements.

Works. The resulting gauge was mounted flush with the surface on the bottom wall and was located a distance 2.54 cm from the end block. A temperature change caused a change in the resistance of the platinum film and the corresponding voltage was recorded during the piston compression (cf. Fig. 1). The resistance thermometer was calibrated in a thermally controlled enclosure so that the wall temperature variation could then be determined from the voltage output. The value of the resulting heat flux is dependent on the parameter $(\rho ck)^{1/2}$ of the insulating ceramic base. This value is $0.033\,\mathrm{cal/cm^2\,^\circ C\,s^{1/2}}$ ($0.138\,\mathrm{W\,s^{1/2}/cm^2\,K}$) for Macor [7].

ANALYSIS

The determination of the heat transfer during piston compression is based on the measured surface temperature of a thermally infinite solid (Macor) that is initially at a constant temperature, T_i. The solution for the wall heat flux is then given by [14]

$$q_{w,s} = \left(\frac{k\rho c}{\pi}\right)^{1/2} \int_0^t \frac{1}{(t-\bar{t})^{1/2}} \frac{\mathrm{d}T_w}{\mathrm{d}\bar{t}}\,\mathrm{d}\bar{t}, \tag{1}$$

which can also be written in the following form [14]:

$$q_{w,s} = \left(\frac{k\rho c}{\pi}\right)^{1/2} \left\{\frac{T_w(t)-T_i}{t^{1/2}} + \frac{1}{2}\int_0^t \frac{T_w(t)-T_w(\bar{t})}{(t-\bar{t})^{3/2}}\,\mathrm{d}\bar{t}\right\}. \tag{2}$$

Note that equation (2) does not require the measurement of slopes. Equations (1) or (2) provide results for the heat flux that are independent of any assumptions concerning the transport processes or conditions in the gas. This will prove to be especially important in confirming the validity of different heat-transfer analyses and mechanisms in the gas.

An alternative approach for the determination of the wall heat flux is based on a solution of the conservation equations in the gas as applied to the thin boundary layer near the wall. Neglecting viscous dissipation and taking the pressure to be uniform yields the following one-dimensional equations of continuity and energy:

$$\frac{\partial \rho}{\partial t} + \frac{\partial(\rho u)}{\partial x} = 0, \tag{3}$$

$$\rho c_p\left(\frac{\partial T}{\partial t} + \frac{u\partial T}{\partial x}\right) = \frac{\mathrm{d}p_\infty}{\mathrm{d}t} + \frac{\partial}{\partial x}\left(k\frac{\partial T}{\partial x}\right), \tag{4}$$

where x is the coordinate perpendicular to the wall. For the end wall configuration x coincides with the direction of piston travel; for the side wall configuration x is perpendicular to the direction of piston travel. It is emphasized that the density increase from the edge of the boundary layer to the wall means that there must be a gas flow towards the wall. This is true for the side walls as well as for the end wall and may be directly affirmed by integrating the equation of continuity to obtain

$$\rho u = -\frac{\partial}{\partial t}\int_0^x \rho\,\mathrm{d}x. \tag{5}$$

It is noted that this induced velocity would also occur when there is no so-called piston velocity present, the motion being a result of the drop in the gas temperature at the wall and the associated increase in density as noted above. For example, reference may also be made to [16] and the references therein where the reflection of a shock wave from a wall is studied. For this problem the cooling effect of the solid also extends into the gas (boundary layer) and the flow of the gas towards the wall is induced in the same manner that is noted above. As a consequence of this effect there is the convective transport of energy, $\rho c_p u(\partial T/\partial x)$, towards the wall [cf. equation (4)].

To solve equations (3) and (4) the stream coordinate ψ is first introduced according to

$$\frac{\rho}{\rho_i} = \frac{\partial \psi}{\partial x}, \quad \frac{\rho u}{\rho_i} = -\frac{\partial \psi}{\partial t}, \tag{6}$$

which satisfies the continuity equation. Then using the ideal gas law, $p_\infty = \rho RT$ and a linear thermal conductivity variation with respect to temperature, the energy equation becomes in ψ,t coordinates (Isshiki and Nishiwaki [4]):

$$\frac{\partial T}{\partial t} = \frac{\gamma-1}{\gamma}\frac{T}{p_\infty}\frac{\mathrm{d}p_\infty}{\mathrm{d}t} + \alpha_i \frac{p_\infty}{p_i}\frac{\partial^2 T}{\partial \psi^2}. \tag{7}$$

Making the transformation $\mathrm{d}\tau = (p_\infty/p_i)\mathrm{d}t$ [4], assuming the gas outside the boundary layer under-

goes an isentropic process* so that

$$\frac{p_\infty}{p_i} = \left(\frac{T_\infty}{T_i}\right)^{\gamma/(\gamma-1)} \tag{8}$$

and introducing the dependent variable $\phi = T/T_\infty$ yields [4]

$$\frac{\partial\phi}{\partial\tau} = \alpha_i \frac{\partial^2\phi}{\partial\psi^2}. \tag{9}$$

The initial and boundary conditions are:

$$\begin{aligned} &\phi(\psi, 0) = 1, \\ &\phi(0, \tau) = T_w/T_\infty = T_w/T_i(V_i/V)^{\gamma-1} = \phi_w. \\ &\phi(\infty, \tau) = 1. \end{aligned} \tag{10}$$

Note that the wall location corresponds to $\psi = 0$. The solution for the wall heat flux is then given by

$$\begin{aligned} q_{w,g} &= +k_w \left.\frac{\partial T}{\partial X}\right|_{x=0} \\ &= -\frac{k_w\rho_w T_\infty}{\rho_i(\pi\alpha_i)^{1/2}} \int_0^\tau \frac{1}{(\tau-\bar{\tau})^{1/2}} \frac{\mathrm{d}\phi_w}{\mathrm{d}\bar{\tau}}\,\mathrm{d}\bar{\tau} \end{aligned} \tag{11}$$

or

$$\begin{aligned} q_{w,g} = -\frac{k_w\rho_w T_\infty}{\rho_i(\pi\alpha_i)^{1/2}} \Bigg[&\frac{\phi_w(\tau)-1}{\tau^{1/2}} \\ &+ \frac{1}{2}\int_0^\tau \frac{\phi_w(\tau)-\phi_w(\bar{\tau})}{(\tau-\bar{\tau})^{3/2}}\,\mathrm{d}\bar{\tau}\Bigg]. \end{aligned} \tag{12}$$

RESULTS AND DISCUSSION

In our previous study [7] experiments were carried out with the thin film gauge placed at the end wall of the compression chamber. Results for the unsteady heat flux from both the conduction relation in the solid, equation (2) for $q_{w,s}$ and from the laminar boundary-layer equations of continuity and energy, equation (12) for $q_{w,g}$, were in very good agreement. This also proves to be true for side wall measurements that have been carried out and typical results are shown in Figs. 2 and 3 for air and argon, respectively. Calculations were also carried out for constant and for time varying values of the wall temperature, but because the variation of the wall temperature was small in comparison to the much larger variation of T_∞, the results were essentially the same. Consequently, the heat flux, $q_{w,g}$, may also be obtained by making the approximation $\phi_w(\tau) \equiv T_w(\tau)/T_\infty(\tau) \simeq$ constant$/T_\infty(\tau)$ so that equation (12) becomes

$$\begin{aligned} q_{w,g} = \frac{-k_w\rho_w}{\rho_i(\pi\alpha_i)^{1/2}} \Bigg\{ &\frac{T_w - T_\infty(\tau)}{\tau^{1/2}} \\ &+ \frac{T_\infty(\tau)T_w}{2}\int_0^\tau \frac{T_\infty^{-1}(\tau) - T_\infty^{-1}(\bar{\tau})}{(\tau-\bar{\tau})^{3/2}}\,\mathrm{d}\bar{\tau}\Bigg\}. \end{aligned} \tag{13}$$

It is emphasized that when the wall temperature variation is small the heat flux, $q_{w,g}$, is determined solely from the variation of $T_\infty(\tau)$. Under this condition, that is, $T_w \simeq T_i$, equation (13) may also be written in terms of the variation of the volume $V(\tau)$ of the compressed gas; namely

$$\begin{aligned} q_{w,g} = \frac{-k_w\rho_w T_i}{\rho_i(\pi\alpha_i)^{1/2}} \Bigg(&\frac{1-(V_i/V)^{\gamma-1}}{\tau^{1/2}} \\ &+ \frac{1}{2}\int_0^\tau \frac{\{1-[V(\bar{\tau})/V(\tau)]^{\gamma-1}\}\,\mathrm{d}\bar{\tau}}{(\tau-\bar{\tau})^{3/2}}\Bigg). \end{aligned} \tag{14}$$

Note that $\rho_w/\rho_i \simeq p_w/p_i$.

Results were also obtained by solving the explicit finite difference forms of the conservation equations in the solid and in the gas. The solution was obtained by matching the temperature and the flux at the wall subject to the required conditions at $\pm\infty$ given by $T(-\infty, t) = T_i$ and $T(+\infty, t) = T_\infty(t)$. The results for the heat flux obtained by this method (not presented) are in very good agreement with the values of $q_{w,g}$. Typical results for the temperature

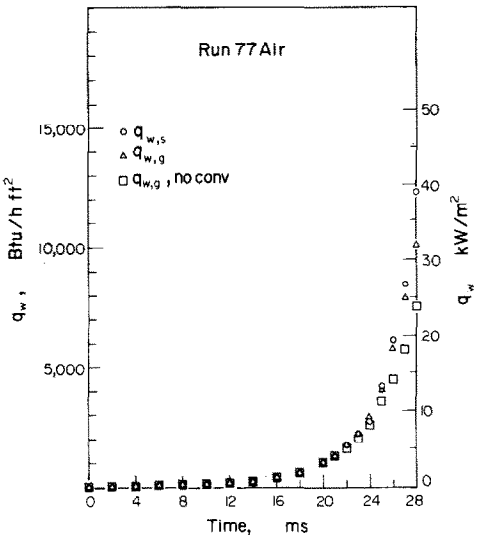

FIG. 2. Heat flux variation.

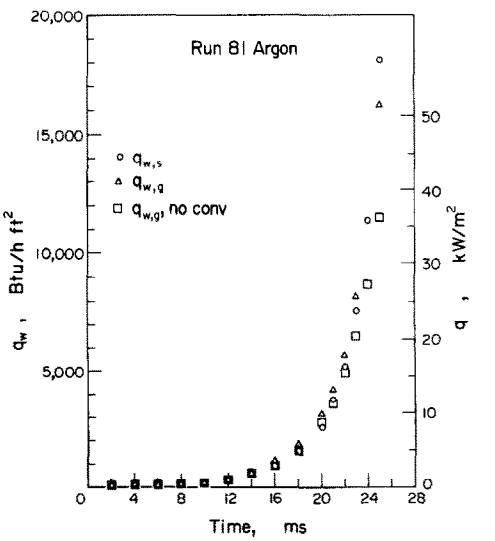

FIG. 3. Heat flux variation.

* It is noted that the measured values of the pressure and the values that were calculated from the isentropic relation for constant specific heats, namely pV^γ = constant, were in very good agreement.

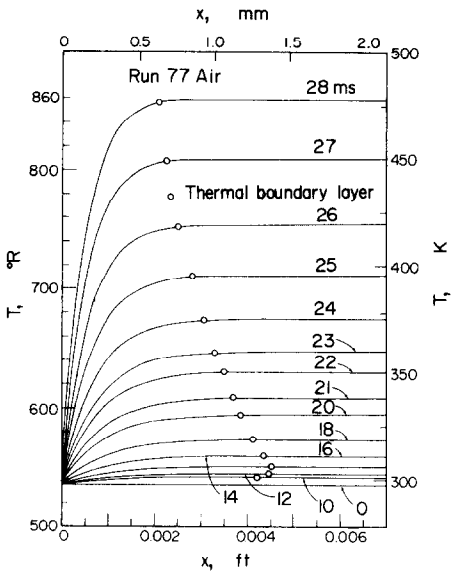

FIG. 4. Temperature profiles in the gas.

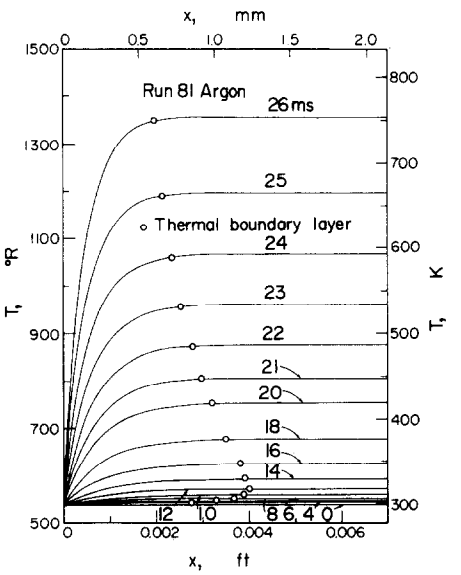

FIG. 5. Temperature profiles in the gas.

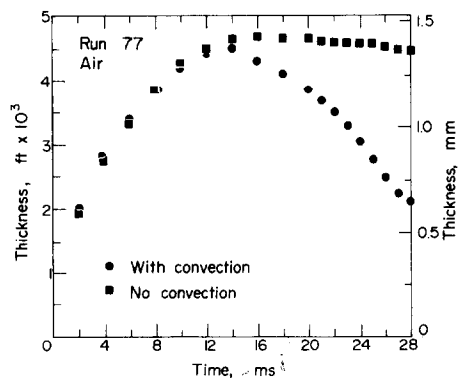

FIG. 6. Thermal boundary layer thickness.

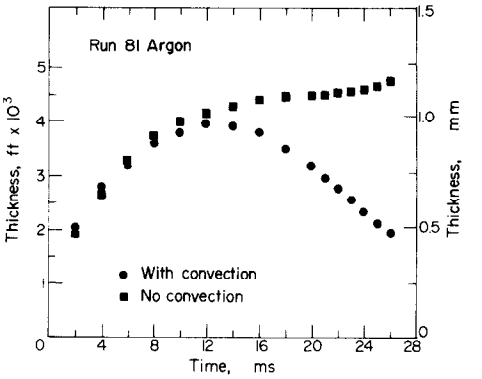

FIG. 7. Thermal boundary layer thickness.

profiles in the gas are given in Figs. 4 and 5. Note that the thermal boundary-layer thickness δ_{th} characterized by the locus of points corresponding to $(T - T_w)/(T_\infty - T_w) = 0.99$, first increases with time but as the compression continues, a maximum value is reached and there is then a decrease with time. A separate plot of the thermal boundary layer δ_{th} is presented in Figs. 6 and 7 along with other results that are discussed below. The velocity profile, $u(x, t)$, was also determined according to

$$u = \frac{-\rho_i}{\rho}\frac{\partial \psi}{\partial t} = \frac{-T}{T_i}\left(\frac{T_\infty}{T_i}\right)^{-\gamma/(\gamma-1)}\frac{\partial \psi}{\partial t} \qquad (15)$$

and these results are presented in Figs. 8 and 9.

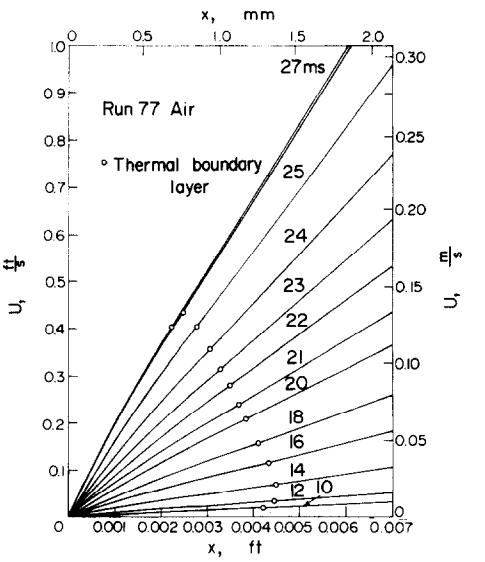

FIG. 8. Velocity profiles in the gas.

The variation of the heat-transfer coefficient is also of interest and the results for $h_s = q_{w,s}/(T_\infty - T_w)$ and $h_g = q_{w,g}/(T_\infty - T_w)$ are shown in Figs. 10 and 11. It is seen that the heat-transfer coefficients first decrease with time, but as the compression continues h_s and h_g reach a minimum value and then increase with time. The large discrepancies at small times are due to inaccuracies associated with both the small heat fluxes and the small temperature differences. The

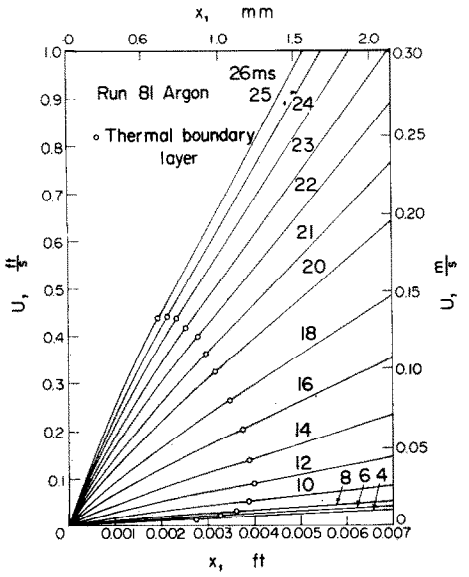

FIG. 9. Velocity profiles in the gas.

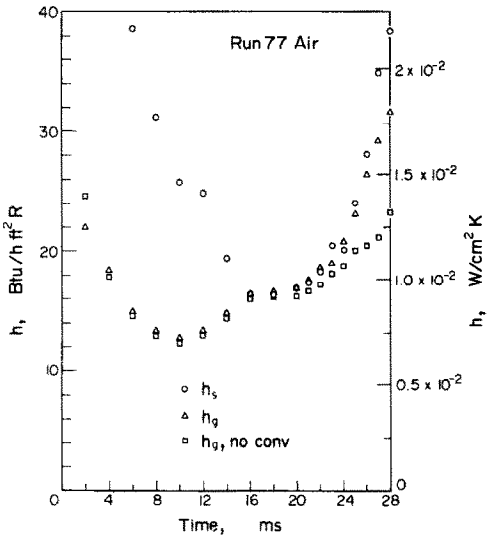

FIG. 10. Heat-transfer coefficient variation.

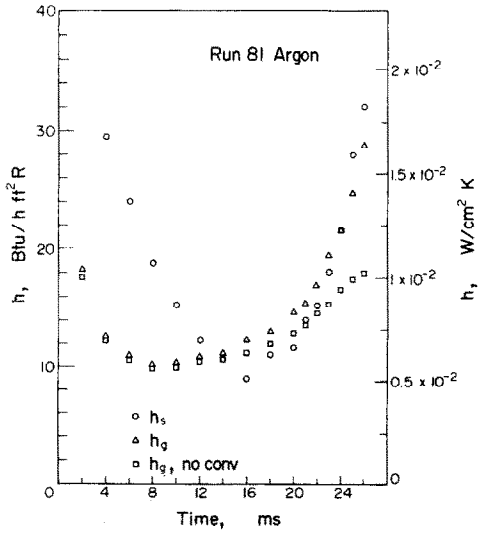

FIG. 11. Heat-transfer coefficient variation.

Table 1. Volume of the compressed gas as a function of time ($V_i = 230.2\,\text{cm}^3$)

Time (ms)	V_i/V Air Run 77	V_i/V Argon Run 81
0	1.000	1.000
2	1.005	1.008
4	1.011	1.017
6	1.017	1.028
8	1.023	1.041
10	1.032	1.064
12	1.045	1.101
14	1.071	1.162
16	1.119	1.260
18	1.194	1.417
20	1.307	1.663
21	1.387	1.844
22	1.492	2.082
23	1.627	2.391
24	1.810	2.799
25	2.069	3.328
26	2.431	4.017
27	2.858	
28	3.335	

variation of the heat-transfer coefficients is discussed below. For completeness, the piston trajectory, $V_i/V(t)$, is presented in Table 1.

To appraise the significance of the convective transport, that is, the effect of the induced velocity on the energy transport, the energy equation was written without the convective term, viz:

$$\rho c_p \frac{\partial T}{\partial t} = \frac{\mathrm{d}p_\infty}{\mathrm{d}t} + \frac{\partial}{\partial x}\left(k\frac{\partial T}{\partial x}\right). \tag{16}$$

Utilizing the ideal gas law, the isentropic relation for the gas outside the boundary layer and a linear thermal conductivity variation with respect to the temperature yields

$$\frac{\partial}{\partial t}\left(\frac{T}{T_\infty}\right) = \alpha_i\left(\frac{T_\infty}{T_i}\right)^{(\gamma-2)/(\gamma-1)} \cdot \times\left(\frac{T}{T_\infty}\right)\frac{\partial}{\partial x}\left[\frac{T}{T_\infty}\frac{\partial}{\partial x}\left(\frac{T}{T_\infty}\right)\right]. \tag{17}$$

Now, introducing the variable $\theta = (T/T_\infty)^2$ and the transformed time $\mathrm{d}\tau = (T_\infty/T_i)^{(\gamma-2)/(\gamma-1)}\mathrm{d}t$ one obtains

$$\frac{\partial\theta}{\partial\tau} = \alpha_i\theta\frac{\partial^2\theta}{\partial x^2}, \tag{18}$$

subject to the following conditions:

$$\begin{aligned}\theta(x,\tau=0) &= 1,\\ \theta(x=\infty,\tau) &= 1,\\ \theta(x=0,\tau) &= (T_w/T_\infty)^2.\end{aligned} \tag{19}$$

The non-linear energy equation was solved numerically using the explicit finite difference method and the results for the heat flux, $q_{w,g,\,\text{no conv}}$, are presented in Figs. 2 and 3. The contribution to the energy transport resulting from the induced velocity corresponds to the difference in the heat fluxes, $q_{w,g} - q_{w,g,\,\text{no conv}}$ and increases with time.

The results for the temperature profiles without convection have not been presented but it is of interest to observe the variation of the thermal boundary-layer thickness $\delta_{th,\,\text{no conv}}$ (cf. Figs. 6 and 7). It is seen that $\delta_{th,\,\text{no conv}}$ continues to increase with time tending to level off at the end of the stroke. This is in contrast to the variation of the thermal boundary-layer thickness with convection, δ_{th}, which increased, reached a maximum value and then decreased with time. A heat-transfer coefficient, $h_{g,\,\text{no conv}} = q_{w,g,\,\text{no conv}}/(T_\infty - T_w)$ has also been calculated and the results are plotted in Figs. 10 and 11. In contrast to the variation of the boundary-layer thickness, $\delta_{th,\,\text{no conv}}$, the variation of $h_{g,\,\text{no conv}}$ (as well as that of h_s and h_g) is a non-monotonic function of time. Indeed, at the beginning of the compression the increase in the boundary-layer thickness with time causes the heat-transfer coefficients to decrease. However, as the compression continues the work done by the piston and the induced convective transport* become more important, finally causing the heat transfer coefficients to increase as shown in Figs. 10 and 11. This is true for both air and argon as the working gas and for both side wall and end wall measurements.

It is also pointed out that there is a contribution to the energy transport that is directly related to the piston velocity. This effect is included in the result for the heat flux from the conduction analysis in the solid ($q_{w,s}$) via the measured wall temperature variation. However, in the boundary layer conservation equations in the gas this contribution, which would correspond to a $\rho c_p v(\partial T/\partial y)$ term, has been omitted. Also omitted in the boundary-layer equations is a mixing effect resulting from the vortex that forms at the piston wall interface [8, 19, 20]. These omissions are consistent with the slightly smaller results for $q_{w,g}$. For completeness, it is noted that these effects should be more pronounced for gauge locations that are farther from the end wall; that is, closer to the piston.

Lastly, calculations were also carried out with a steel wall for the piston trajectories corresponding to run 77 for air and run 81 for argon. The results were obtained by matching the temperature and the flux at the surface subject to the required conditions at $\pm\infty$ given by $T(-\infty, t) = T_i$ and $T(+\infty, t) = T_\infty(t)$. For these cases the wall temperature variation was again small, so that $T_w \approx T_i$ and the results were substantially the same as previously presented. For completeness, it is noted that the heat flux was slightly larger for the steel wall.

CONCLUSIONS

The unsteady heat transfer to the side walls during the piston compression of a single stroke may be determined from the solution of the laminar boundary layer equations in the gas. For small wall temperature variations, the heat flux may be determined solely from the variation of the temperature outside the boundary layer, T_∞ or alternatively, from the piston trajectory in the form of the volume of the compressed gas as a function of time. Results for the heat-transfer coefficient for air and argon exhibit a non-monotonic variation with respect to time. The results for the side wall measurements are in agreement with measurements that were previously made at the end wall.

Acknowledgement –The authors acknowledge with appreciation the support of this research by the National Science Foundation under HSF/RANN Grant AER-76-08727 and by the U.S. Department of Energy under Contract W-7405-ENG-48.

*The convective transport contribution is only relevant to h_s and h_g since it is defined to be zero for the hypothetical $h_{g,\,\text{no conv}}$ analysis.

REFERENCES

1. H. Pfriem, Zur messung schnell wechselnder temperatures in des zylinderwand von kolbenmaschiesen, *Forschung Ing.-West* **6**(4), 195–201 (1935).
2. V. D. Overbye, J. E. Bennethum, O. A. Uyehara and P. J. Myers, Unsteady heat transfer in engines, *Trans. Soc. Auto. Engrs* **69**, 461–494 (1961).
3. W. J. D. Annand, Heat transfer in the cylinders of reciprocating internal combustion engines, *Proc. Inst. Mech. Engrs* **177**, 973–996 (1963).
4. N. Isshiki and N. Nishiwaki, Study on laminar heat transfer of inside gas with cyclic pressure change on an inner wall of a cylinder head, *Proceedings of the 4th International Heat Transfer Conference*, FC3.5, pp. 1–10. Paris–Versailles (1970).
5. K. Dao, O. A. Uyehara and P. S. Myers, Heat transfer rates at gas–wall interfaces in motored piston engines, *Trans. Soc. Auto. Engrs* **82** (730632), 2237–2258 (1974).
6. M. S. Chong, E. E. Milkins and H. C. Watson, The prediction of heat and mass transfer during compression and expansion in I.C. engines, *Trans. Soc. Auto. Engrs* **84**, 760761 (1976).
7. M. Nikanjam and R. Greif, Heat transfer during piston compression, *J. Heat Transfer* **100**, 527–530 (1978).
8. A. K. Oppenheim, R. K. Chang, K. Teichman, O. I. Smith, R. F. Sawyer, K. Ham and H. E. Stewart, A cinematographic study of combustion in an enclosure filled with a reciprocating piston, in *Conference on Stratified Charge Engines*, London, England (1976).
9. A. Meier, Recording rapidly changing cylinder-wall temperatures, translation, NACA TM 1013 (1939).
10. J. Rabinowicz, M. E. Jessey and C. A. Bartsch, Resistance thermometer for heat transfer measurement in a shock tube, GALCIT Hypersonic Research Project Memo, 33, Guggenheim Aeronautical Laboratory, California Institute of Technology, July (1956).
11. R. Vidal, Model instrumentation techniques for heat transfer and force measurements in a hypersonic shock tunnel, Report AD 917-A-1, Buffalo, N.Y., Cornell Aeronautical Laboratory, Inc. (1956).
12. R. Bromberg, Use of the shock tube wall boundary layer in heat transfer studies, *Jet Propulsion* **26**, 737–740 (1956).
13. P. H. Rose and W. I. Stark, Stagnation point heat transfer measurements in air at high temperature, Research Note 24, Everett, Mass., AVCO Research Laboratory, AVCO Manufacturing Corp. December (1956).
14. J. G. Hall and A. Hertzberg, Recent advances in transient surface temperature thermometry, *Jet Propulsion* **28**, 719–723 (1958).

15. L. Bogdan, High-temperature, thin-film resistance thermometers for heat transfer measurement, NASA Contractor Report, NASA CR-26 April (1964).
16. D. J. Collins, R. Greif and A. E. Bryson, Measurements of the thermal conductivity of helium in the temperature range 1600–6700 K, *Int. J. Heat Mass Transfer* **8**, 1209–1216 (1965).
17. D. J. Collins, Shock tube study for the determination of the thermal conductivity of neon, argon and krypton, *J. Heat Transfer* **88C**, 52–56 (1966).
18. G. T. Skinner, Calibration of the thin-film gauge backing materials, *ARS J.* **31** (1961).
19. R. J. Tabaczynski, D. P. Hoult and J. C. Keck, High Reynolds number flow in a moving corner, *J. Fluid Mech.* **42**, 249–256 (1970).
20. H. Daneshyar, D. E. Fuller and B. E. L. Decker, Vortex motion induced by the piston of an internal combustion engine, *Int. J. Mech. Sci.* **15**, 381–390 (1973).

TRANSFERT THERMIQUE PENDANT LA COMPRESSION PAR PISTON EN INCLUANT LA TEMPERATURE DE LA PAROI ET LES EFFETS DE CONVECTION

Résumé—Le flux thermique instationnaire entre un gaz inerte et les parois d'un canal a été déterminé pendant la compression pour une course de piston. Pour des petits changements de température de paroi, le flux thermique peut être déterminé uniquement à partir de la variation de la température hors de la couche limite ou bien à partir du mouvement du piston. On présente aussi des résultats pour le coefficient de transfert thermique et on montre une variation non monotone en fonction du temps.

WÄRMEÜBERGANG BEI EINER KOLBENKOMPRESSION UNTER BERÜCKSICHTIGUNG VON ZYLINDERWAND- UND KONVEKTIONSEFFEKTEN

Zusammenfassung—Der instationäre Wärmestrom eines nicht-reagierenden Gases an die Seitenwände eines Kanals wurde bei der Kolbenkompression für einen einzelnen Hub bestimmt. Für kleine Wandtemperaturänderungen kann der Wärmestrom allein durch die Variation der Temperatur auß erhalb der Grenzschicht oder alternativ durch die der Kolbenlauffläche bestimmt werden. Es werden Ergebnisse für den Wärmeübergangskoeffizienten angegeben, die eine nicht-monotone Änderung mit der Zeit zeigen.

ТЕПЛОПЕРЕНОС ПРИ РАБОЧЕМ ХОДЕ ПОРШНЯ С УЧЁТОМ ВЛИЯНИЯ БОКОВЫХ СТЕНОК ЦИЛИНДРА И КОНВЕКЦИИ

Аннотация — Определена величина нестационарного переноса тепла от нереагирующего газа к боковым стенкам цилиндра в течение одного рабочего хода поршня. При небольших изменениях температуры стенок цилиндра величина теплового потока может быть определена только на основании изменения температуры за пределами пограничного слоя или из траектории хода поршня. Приведены результаты расчётов коэффициента теплопереноса и показано, что значения коэффициента немонотонно изменяются во времени.